Thin Solid Films 707 (2020) 138068

Contents lists available at ScienceDirect

Thin Solid Films

journal homepage: www.elsevier.com/locate/tsf

Selective crack formation on stretchable silver nano-particle based thin films for customized and integrated strain-sensing system

Seongdae Choi, Seunghwan Lee, Byeongmoon Lee, Taehoon Kim*, Yongtaek Hong

Department of Electrical and Computer Engineering, Inter-University Semiconductor Research Center (ISRC), Seoul National University, Seoul 08826, Republic of Korea

ARTICLE INFO

Keywords:
Inkjet-printing process
Silver nano-particle based thin film
Crack-based strain sensor
Integrated strain sensing system
Customizable wearable device

ABSTRACT

Wrinkle structure effectively suppresses the crack formation in a material under tensile strain, thus enabling intrinsically brittle material to be strain-tolerant. If the brittle nature of the material can be selectively engineered on the wrinkle structure, combination of mechanically different structures can be obtained within the same material. In this work, we introduce a simple and facile approach to effectively turn strain-tolerant conductive metal thin film with wrinkle structure into crack-rich thin film. The intended phenomenon was controlled by additionally inkjet-printing Ag thin film onto the wrinkle structure, and the structure and performance were also systematically optimized to enhance sensitivity and stability of the sensor. Our strategy to induce intended cracks on corrugated metal thin film enables not only to stably combine stretchable interconnectors and strain sensors but also to fabricate an integrated strain sensor system that can be custom-tailored to the subject's hand size. We believe the facile strategy will be a good step to realize an integrated strain sensor system.

1. Introduction

Recently, stretchable electronics [1–3] has attracted great interest for the next generation electronic devices owing to their high feasibility with surrounding environment. Integrated systems composed of various device components exhibit excellent performances for interesting bio-inspired areas such as health-monitoring [1,4] and human motion detecting [4–6] applications. To practically realize the use of stretchable electronic devices, it is important that the integration of each component should be durable and reliable under harsh conditions.

Strain sensor is one of the most popular components in the stretchable electronic devices. Previous role of strain sensor has been confined to detecting vibration or small-level expansion and typically used in the macro-scale civil engineering [7]. However, over the past decades, the facile use of strain sensor has been continuously involved in the stretchable electronics, as the strain sensor with high flexibility can be attached on human body and detect various human motions with wide range of strain signals such as jumping, finger-bending and grasping. Consequently, a number of research groups have reported interesting flexible strain sensors which utilized cracking phenomenon on various conductive materials to accomplish high strain-sensitivity [3,6,8–15]. The electrical resistance of the crack-based strain sensor varies according to the opening of microcracks that are generated on brittle conductive films by the applied tensile strain. However, as the systematic integration of interconnecting line and strain sensor at high-level strain loading is still a huge challenge, the stretchable sensors should be reliable under high-level deformation. Furthermore, although all component parts are fabricated to be stable against the external deformation, it is still difficult to develop strain-tolerant interface between interconnection line and strain sensor. The poor interface causes not only a severe error but also low reliability of the entire sensor system. To overcome this issue, the eutectic liquid metal has been used for the conducting interface between device and interconnection, but it is not able to be widely utilized due to its intrinsic phase transition effect [16]. In addition, although composite-based integration using carbon nanomaterials has high reliability, it is hard to design a complex configuration that consists of narrow and long interconnector owing to its high resistance level [16]. Therefore, a facile strategy to use highly conductive materials should be addressed for various and complex configurations.

Silver nanoparticles (Ag NPs) is one of the most useful materials for various stretchable applications for its good conductivity and solution-process availability [1,17–20]. However, the Ag NPs based thin film is intrinsically brittle and heavily vulnerable to the external strain. Therefore, the easy use of silver (Ag) material for stretchable applications has been mainly resulted from some extrinsic stress-releasing

* Corresponding authors.
E-mail addresses: sd0690@snu.ac.kr (S. Choi), shree1989@snu.ac.kr (S. Lee), hardrist@snu.ac.kr (B. Lee), rhlight4@snu.ac.kr (T. Kim), yongtaek@snu.ac.kr (Y. Hong).

https://doi.org/10.1016/j.tsf.2020.138068
Received 3 December 2019; Received in revised form 21 April 2020; Accepted 21 April 2020
Available online 11 May 2020
0040-6090/

wrinkle structures [18,20–24]. While, if the vulnerable nature can be selectively evoked in the intended area on the wrinkle structure, mechanically different structures of wrinkle and crack-rich regions can coexist. Accordingly, based on the different strain-responses of each structure, they can be utilized as stretchable electrode or strain sensor, respectively.

In this study, we implemented an integrated strain sensor system which consists of strain sensor and stretchable line on a stretchable polydimethylsiloxane (PDMS) substrate by inkjet-printing Ag ink. The stretchable Ag line has the wrinkled structure which enables the brittle Ag line to be durable and reliable up to specific strain through fold-unfolding behavior. By inkjet-printing additional Ag layer onto the specific area of the wrinkle structure, the easily patternable crack-based Ag strain sensor was fabricated. The strain-responses of each structure were analyzed by measuring the resistance variation and morphological changes under tensile strain, and the sensor performance was optimized to certify high sensitivity and stability. Finally, as the inkjet printing method enabled the customizable configuration of stretchable interconnects and strain sensor, the integrated system was utilized for selectively detecting different joint motion in a hand without interferences.

2. Experimental methods

To fabricate PDMS substrate (thickness: 300 μm), 10:1 weight ratio mixture of PDMS (Sylgard 184 from Dow Corning) and curing agent was spin-coated onto glass substrate, followed by annealing at 120 ˚C for 30 min. After detaching the cured PDMS substrate from the glass, we fixed it onto the stretching equipment, and stretched the elastomer to 100 % strain as shown in Fig. 1(a). To make the surface of PDMS hydrophilic, the surface was treated with UV ozone. Then, Ag NP ink (DGP-40 from ANP Corp.) was inkjet-printed onto the PDMS substrate which was located on a heated plate (60 ˚C), by using a piezo electric inkjet printer (DMP-2831 from Dimatix Corp.) with 21 μm diameter nozzles. The nozzle squirted ~10 pL droplets of the Ag NP ink and the droplet formed a circle with a diameter of ~40 μm on the UV ozone treated PDMS substrate. And the distance between the centers of adjacent droplets was 35 μm. After annealing the sample at 120 ˚C for 30 min, the elongated elastomer was released to flattened state, and wrinkled Ag base layer was formed. Then, Ag NP ink was additionally inkjet-printed onto the specific area of Ag wrinkled film on the heated plate (60 ˚C) to form crack-inducing Ag layer. The distance between the centers of adjacent droplets of Ag ink was 40 μm. After annealing process (120 ˚C for 30 min), the hybrid structured Ag strain sensor was fabricated. Optical measurement for the sensor was performed with scanning electron microscopes (SEM) (S-4800 from HITACHI) to obtain structural data such as surface morphology and crack generation. Moreover, to measure the electrical characteristic of the strain sensor under tensile strain, we fixed the sample to the customized stretching device to apply strain to the sensor. Then, electrical measurement for the sensor was performed with a source meter (Keithley 2400 from Tektronix). The resistivity of the strain sensor was measured by applying voltage of 0.1V throughout the sample.

3. Results and discussion

There are various interesting phenomena about strain-response resulted from structural or morphological change of the materials. In stretchable electronics, capacitive and piezo-resistive types have widely been utilized for stretchable strain sensor. The former has high accuracy, but it is difficult to design their structures on the wearable system because of the metal-insulator-metal structure. The latter has some

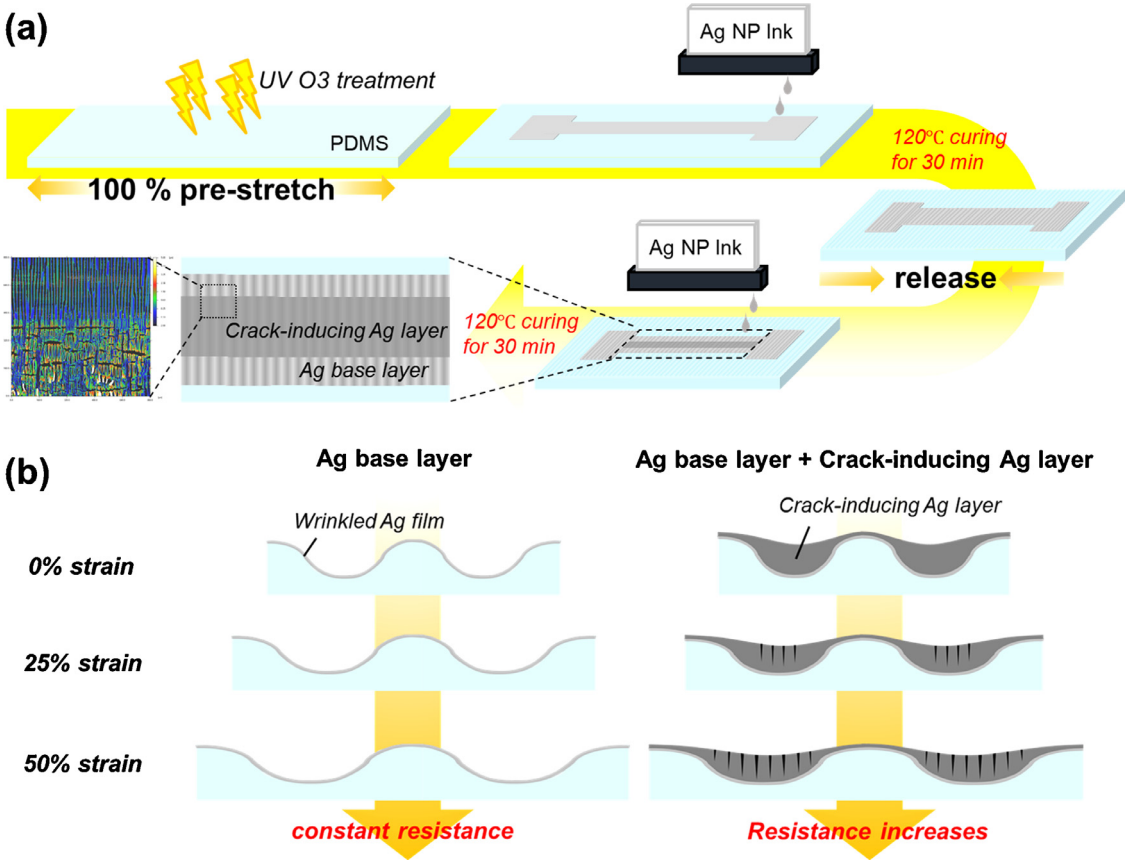

Fig. 1. Schematic illustration of (a) the whole process flow of fabricating Ag strain sensor by inkjet-printing process and (b) working principles of the Ag base layer without or with the crack-inducing Ag layer under tensile strain.

advantages in easy fabrication and the choice of material, but it is hard to simultaneously obtain two sensing performances of strain-sensitivity and reliability. Among the piezo-resistive strain sensors, cracking is one of the most popular phenomena in stretchable electronics [3,13,15,23,25–30]. In general, the factors that determine crack formation are the mechanical properties of the materials and induced strain on the material. So, if stress-releasing structures including wrinkles are well-constructed on the metal materials, crack formation even at high tensile strain can be avoided in spite of their extremely poor mechanical properties. In contrast, highly tough materials with stress-focusing notch structures can be easily fractured even at small strain loading. In previous study, by using selective toughening methodology, different crack formations in same material were obtained, and the two regions (fracture-designed and fiber-reinforced regions) showed different roles on the stretchable strain sensor [13]. It means that selective crack controlling method enables the piezo-resistive strain sensor to have both the strain-sensitivity and reliability by separating the roles.

Ag NPs based thin films on bare elastomer substrate are well known to be fragile even at small external tensile strain, leading to entire channel rupture due to their intrinsically poor ductility under tensile strain [22]. To complement the poor electrical stability, in this study, wrinkle structure of the metal thin film formed by inkjet printing Ag NPs based ink onto the pre-stretched platform was utilized to dissipate the strain energy from elongated platform and lessen the abrupt channel fractures, which allowed the film to be durable at strain loading as shown in Fig. 1(b). Afterwards, by additionally inkjet-printing Ag ink onto the specific area of the wrinkled metal thin film, Ag ink flew down to the valley of the corrugated Ag film before curing process. As a result, thickness-gradient Ag film (crack-inducing Ag layer) was deposited onto the wrinkled film as shown in Fig. 1(b). As cracks are more likely to be generated on the thicker metal film, [31] we were able to generate controlled cracks on the film, which gradually increased electrical resistance under tensile strain. In addition, the sensor's sensitivity will increase with the Ag film thickness. The printed film thickness was ~610, ~809, ~1150, and ~1273 nm for the films formed by one-, two-, three-, and four-time inkjet-printing, respectively. As a result, the whole film is systematically divided into two parts. One is Ag base layer that maintains stable electrical property, and the other is hybrid structured Ag film with additionally printed crack-inducing layer, which leads to a highly sensitive strain-sensing device.

In order to verify the strain-response of the Ag strain sensor, microstructural changes on the metal thin film are optically explained in Fig. 2. The optical images of samples were exhibited at its initial state and 50% strain, respectively. Fig. 2(a) shows the crack-inducing layer which is deposited onto the wrinkled Ag film at 0% strain. It is noted that unintended lateral cracks are generated on the film owing to Poisson's effect of the elastomeric substrate. However, vertically generated cracks that cause change in resistance are not noticed, even on the film where the crack-inducing layer and the base layer meets as shown in Fig. 2(b). On the contrary, as comparably thicker film is supposed to be more easily cracking, complete large cracks are vertically generated on the crack-inducing layer at 50% strain loading, which makes the film be electrically isolated. (Fig. 2(d)) The large cracks gradually decrease in size as the thickness of the Ag sensing film decreases, then accordingly disappear on the wrinkled film as depicted in Fig. 2(e). In addition, as shown in Fig. 2(c) and (f), only micro-scale cracks are seen on the Ag base film under 50% strain, but don't have a significant effect on the noticeable change in electrical resistance.

Based on the morphological analysis, we analyzed the resistance variation of the metal thin film under tensile strain. The stretchable properties of Ag wrinkled base layer that were formed on the pre-stretched elastomer are featured in Fig. 3(a) and (b), and the hybrid structured Ag thin films that includes crack-inducing layer, are shown in Fig. 3(c)-(f), respectively. The extent of the strain which wrinkled base layer can stand without changing electrical resistance is determined by how the elastomer was pre-stretched. Therefore, as shown in Fig. 3(a), Ag base layer that had been implemented on 100% pre-stretched platform maintained constant resistance up to higher strain than that with 50% pre-strain. In addition, as the thickness of metal film increases, the resistance starts to increase slightly earlier and more sharply. As a result, it was certified that single layered Ag film with 100% pre-strain was preferred for the base layer, which assured wide strain range. Furthermore, to certify the mechanical stability of the base layer of 100% pre-strain, cyclic test for 1,000 times was also performed as shown in Fig. 3(b). While the sample showed poor resistance repeatability under 70% strain, the sample showed reliable and durable property when it was repeatedly stretched to 50% strain. Thus, the working range of the strain sensor was determined as 50% strain to meet the mechanical stability. The tension speed of stretching test on base layer was 10mm/min and 100 mm/min for Fig. 3(a) and (b), respectively. In Fig. 3(c)-(f), when it comes to investigate the resistance variation of hybrid structured Ag strain sensor, cyclic tests were performed in harsh conditions (cycling number: 1,000 times, strain range: 50%, tension speed: 100 mm/min). As shown in Fig. 3(c) and (d), the sensor showed higher sensitivity as the number of crack-inducing layers increased from 1 to 3. However, the cyclic repeatability of the sensor was guaranteed up to double layers, as too bulky additional film induced unintended cracks propagated to the base layer. In addition, the sensitivity of the sensor could be enhanced by optimizing the patterned ratio of crack-inducing layer to base layer as shown in Fig. 3(e) and (f). By increasing the ratio up to 50%, the sensor showed higher sensitivity with fairly excellent stability. Here, to quantitatively state the sensitivity of the strain sensor, gauge factor can be analyzed [32, 33], which can be calculated as

$$\text{Gauge factor} = \frac{\Delta R/R_o}{\Delta L/L_o}$$

where R and L denotes the resistance value and the length of the strain sensor, respectively. Thus, the strain sensor with higher sensitivity shows bigger gauge factor as the resistance increases higher when the same strain loading is applied. In conclusion, as single-layered Ag wrinkle film which had been formed at 100% pre-stretched PDMS and double-layered films that were coated on the 50% of the base layer were combined, the strain sensor with high sensitivity (gauge factor ~10) and stability was obtained.

As the wrinkled Ag film has widely been utilized as stretchable interconnects, the strategy of additionally inkjet-printing crack-inducing layer onto the wrinkled Ag film enabled the large-area integrated strain-sensing system. Therefore, in order to show the practical usage of Ag strain sensor, we demonstrated a human motion detecting device which could help measure the joints flexion of finger in Fig. 4. The device is dimensionally customizable to the users of different finger size with the merit of easily patterning additional layer onto the desired region by inkjet-printing process. As depicted in Fig. 4(a), the device, that was conformally attached onto the index finger, consisted of 4 Ag wrinkled lines (**1**~**4**). The common line **1** was electrically connected to the other lines (**2**~**4**) that were parallelly connected one another, and, as a result, 3 Ag stretchable electrodes (**1-2, 1-3, 1-4**) were implemented. Then, additional Ag film was patterned on the specific area of wrinkled electrode, to exactly align with the joints of index finger for the accurate measurement. Each Ag strain sensor which were located on each line **2** and **3**, was supposed to detect the flexion of PIP (Proximal Inter-Phalangeal) joint and MP (Metacarpo-Phalangeal) joint of index finger, respectively, and, '**d**' denotes the distance between the middle points of two strain sensors. The line **4** was for the reference result of Ag wrinkled electrode. In Fig. 4(b), from the distance between PIP and MP joints of users, the device could be dimensionally tailored regardless of the size of their fingers (length between PIP and MP joints of person 'A' and person 'B' are 5 cm and 6.4 cm, respectively). In Fig. 4(c), to analyze the tailoring effect of the device, the device (**d**: 5 cm) showed remarkable change in resistance from the PIP joint flexion

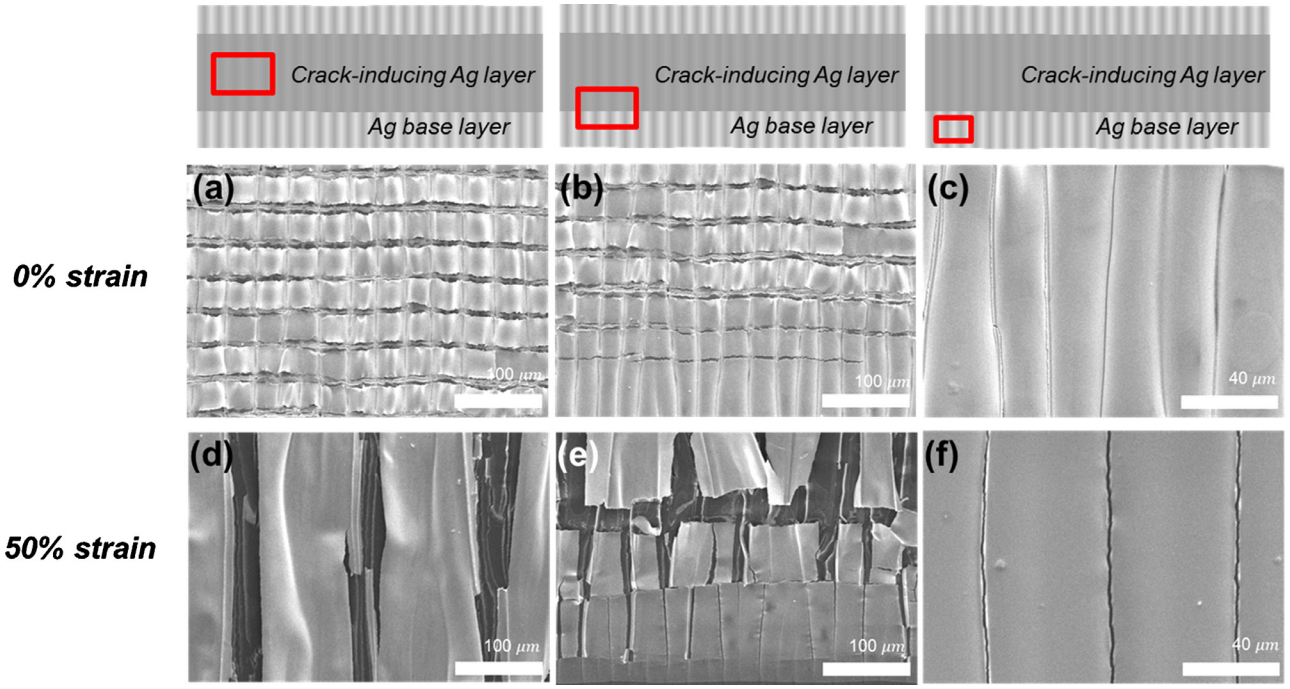

Fig. 2. Optical images of crack generation on the Ag strain sensor scanning from the crack-inducing layer to base layer, at (a-c) 0% strain and (d-f) 50% strain.

(90° degree) of a person whose PIP-MP joint distance was correspondingly 5 cm. On the other hand, the misalignment of the sensors with joints (**d** was either 4 cm or 6 cm) caused the device to malfunction. Moreover, with the high sensitivity and wide working range of strain sensor, excellent performance of the device was observed from the result that the change in resistance linearly increased according to the degree of PIP joint flexion (30°, 60°, 90°) (Fig. 4(d)). It is noted that the measured resistance changed after the finger was bent because there is a mechanical relaxation delay for the viscoelastic PDMS when the bending strain is quickly applied. Similar phenomenon was also reported in other types of piezoresistive strain sensors based on PDMS substrate [34,35]. Finally, as shown in Fig. 4(e), for the integrated strain-sensing device to selectively detect PIP and MP joints of finger, we performed an experiment that verified the ability to distinguish signals from the various flexions of index finger. Through the various movements of index finger (stretching, PIP bending, MP bending and PIP & MP bending) at regular intervals of 5 seconds, it was observed that the resistance variation from each joint flexion was independent without any interference. In addition, compared to the reference line that showed no resistance change under joint flexion, the resistance

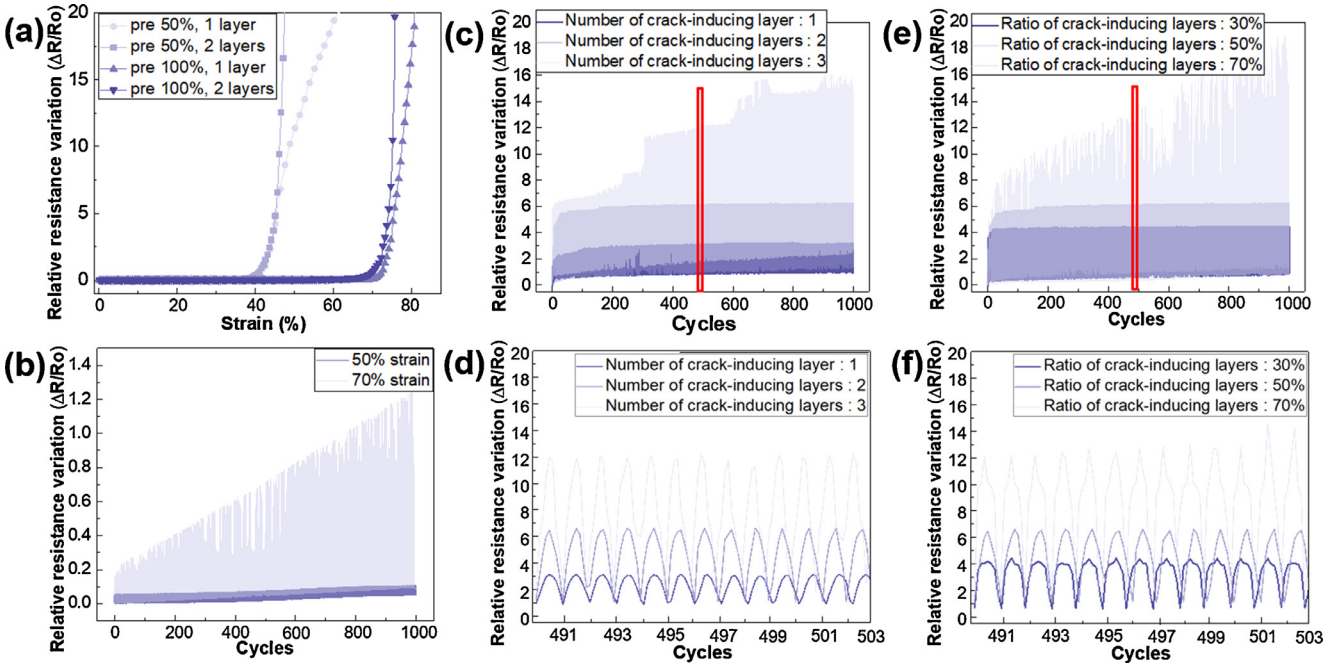

Fig. 3. Electrical resistance variations of (a) base layer according to the extent of pre-strain (50%, 100%) and the number of layers (1, 2) and (b) the repeated cyclic tests (1000 times) of the Ag base layer (pre-strain: 100%) as the function of strain loadings (50%, 70%). Resistance variations in repeated cyclic tests of strain sensor with (c, d) various number (1, 2, 3) and (e, f) ratio (30%, 50%, 70%) of Ag crack-inducing layers.

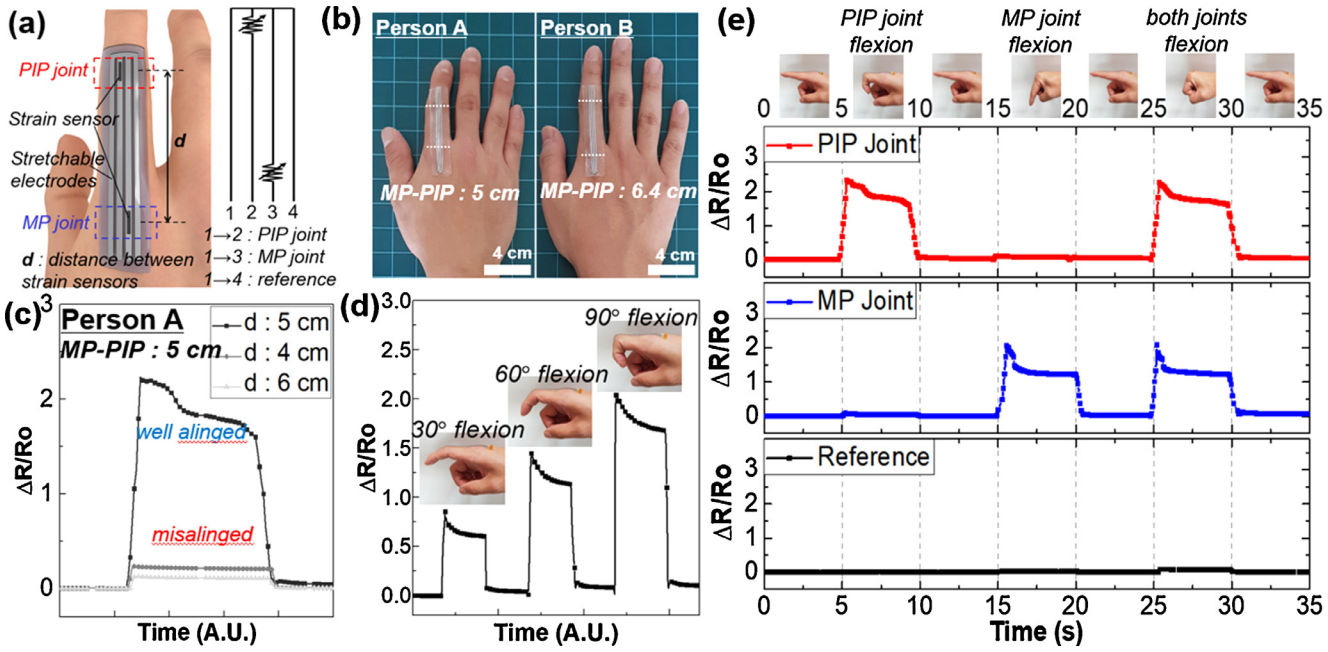

Fig. 4. (a) Schematic depiction of the joint-flexion detecting device (d: distance between strain sensors) and (b) dimensional customization of the device for the users (person A, person B) with different hand size. (c) Resistance variation of the devices of various size (d: 4 cm, 5 cm, 6 cm) by the PIP joint-flexion of Person A (MP-PIP length: 5cm), and (d) resistance variation of the device according to the degree of PIP joint flexion (30˚, 60˚, 90˚). (e) Resistance variation of the device by various movements of index finger in regular sequences.

change of well-aligned Ag strain sensor was further notable.

In order to emphasize the feasibility of the wearable device applicable to real life, we demonstrated the device to accurately detect several common actions with finger movement, which were clicking mouse (Fig. 5(a) and (b)) and grabbing bar (Fig. 5(c)). Detecting mouse clicking motion was conducted in two ways: the resistance variations that were caused by clicking frequently using only the PIP joint, and clicking slowly using only the MP joint are exhibited in Fig. 5(a) and (b), respectively. By selectively monitoring the movement of each finger joint, it was noteworthy that more precise motion detecting of the device was available by subdividing the clicking action that could be regarded as the same motion. Meanwhile, as shown in Fig. 5(c), the resistance variation by repeatedly grasping and releasing bar shows the ability of the device to detect the finger movement with both joints at the same time. Our results well demonstrated the characteristics of Ag strain sensor and the use of integrated strain sensing system as customizable human motion monitoring device application.

4. Conclusions

To summarize, we have presented a Ag NPs based strain sensor by patterning additional layers onto the desired area of the wrinkled Ag film to induce intended crack formation with a facile and low-cost inkjet-printing fabrication process. Thus, the hybrid structured Ag film was systematically divided into two parts to accomplish both sensitivity and reliability of the brittle material based strain sensor. In addition, by optimizing fabrication conditions and structures of the strain sensor, we obtained a stable resistance variation with high gauge factor of ~10 up to 50% tensile strain. Based on the combination of fabricated strain sensor and wrinkle film that can be utilized as Ag stretchable electrode,

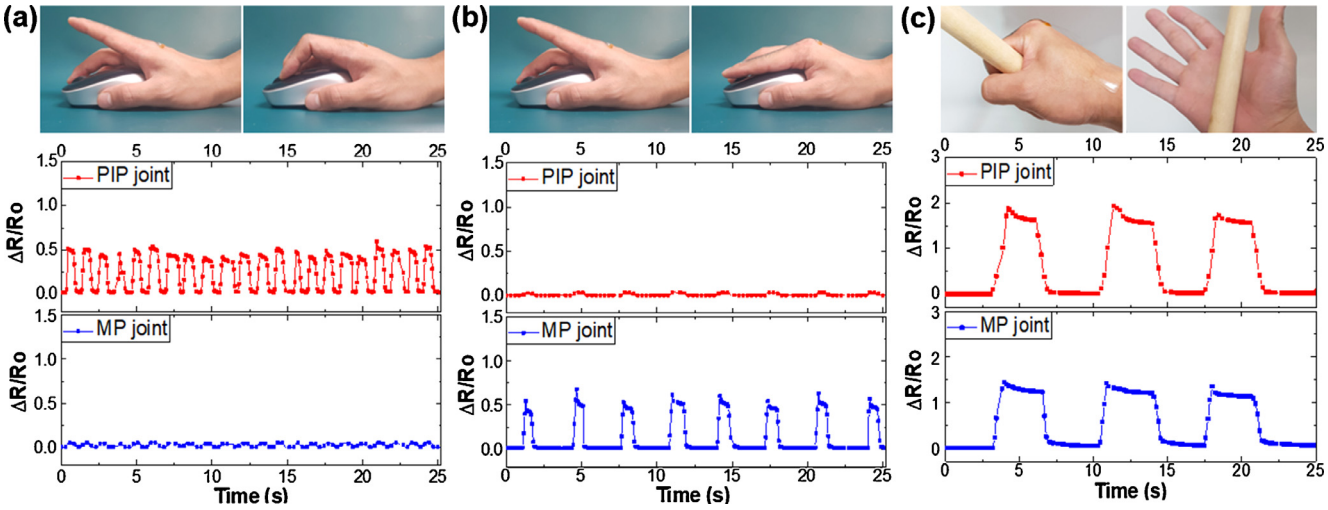

Fig. 5. Resistance variation of the device with various actions of (a) fast mouse-clicking with PIP joint flexion, (b) slow mouse-clicking with MP joint flexion, and (c) grasping and releasing bar.

we demonstrated an integrated strain-sensing system applicable to the human-motion detecting device. The integrated device is able to detect flexion of multiple joints, and it can be dimensionally tailored regardless of users' hand size. It is noted that the selectively crack-inducing strain sensor is applicable to various wearable devices which require accurate measurement of common actions in human life.

CRediT authorship contribution statement

Seongdae Choi: Conceptualization, Methodology, Formal analysis, Investigation, Writing - original draft, Visualization. **Seunghwan Lee:** Conceptualization, Methodology. **Byeongmoon Lee:** Methodology. **Taehoon Kim:** Writing - review & editing. **Yongtaek Hong:** Writing - review & editing, Supervision.

Declaration of Competing Interest

The authors declare that they have no known competing financial interests or personal relationships that could have appeared to influence the work reported in this paper.

Acknowledgments

The research was supported in part by Samsung Electronics and the Industry technology R&D program (20006467) funded By the Ministry of Trade, Industry & Energy (MOTIE, Korea).

References

[1] M. Amjadi, K.U. Kyung, I. Park, M. Sitti, Stretchable, Skin-Mountable, and Wearable Strain Sensors and Their Potential Applications: A Review, Adv. Funct. Mater. 26 (2016) 1678–1698, https://doi.org/10.1002/adfm.201504755.

[2] C.L. Choong, M.B. Shim, B.S. Lee, S. Jeon, D.S. Ko, T.H. Kang, J. Bae, S.H. Lee, K.E. Byun, J. Im, Y.J. Jeong, C.E. Park, J.J. Park, U.I. Chung, Highly stretchable resistive pressure sensors using a conductive elastomeric composite on a micropyramid array, Adv. Mater. 26 (2014) 3451–3458, https://doi.org/10.1002/adma.201305182.

[3] D. Kang, P.V. Pikhitsa, Y.W. Choi, C. Lee, S.S. Shin, L. Piao, B. Park, K.Y. Suh, T.I. Kim, M. Choi, Ultrasensitive mechanical crack-based sensor inspired by the spider sensory system, Nature 516 (2014) 222–226, https://doi.org/10.1038/nature14002.

[4] Y.J. Liu, W.T. Cao, M.G. Ma, P. Wan, Ultrasensitive wearable soft strain sensors of conductive, self-healing, and elastic hydrogels with synergistic "soft and hard" hybrid networks, Acs Appl Mater Inter 9 (2017) 25559–25570, https://doi.org/10.1021/acsami.7b07639.

[5] Y.C. Ding, J. Yang, C.R. Tolle, Z.T. Zhu, A highly stretchable strain sensor based on electrospun carbon nanofibers for human motion monitoring, Rsc. Adv. 6 (2016) 79114–79120, https://doi.org/10.1039/c6ra16236c.

[6] J. Lee, S. Kim, J. Lee, D. Yang, B.C. Park, S. Ryu, I. Park, A stretchable strain sensor based on a metal nanoparticle thin film for human motion detection, Nanoscale 6 (2014) 11932–11939, https://doi.org/10.1039/c4nr03295k.

[7] P. Moyo, J.M.W. Brownjohn, R. Suresh, S.C. Tjin, Development of Fiber Bragg grating sensors for monitoring civil infrastructure, Eng. Struct. 27 (2005) 1828–1834, https://doi.org/10.1016/j.engstruct.2005.04.023.

[8] Q. Li, H. Liu, S. Zhang, D. Zhang, X. Liu, Y. He, L. Mi, J. Zhang, C. Liu, C. Shen, Superhydrophobic electrically conductive paper for ultrasensitive strain sensor with excellent anticorrosion and self-cleaning property, ACS Appl. Mater. Interfaces 11 (2019) 21904–21914, https://doi.org/10.1021/acsami.9b03421.

[9] H. Liu, Q. Li, Y. Bu, N. Zhang, C. Wang, C. Pan, L. Mi, Z. Guo, C. Liu, C. Shen, Stretchable conductive nonwoven fabrics with self-cleaning capability for tunable wearable strain sensor, Nano Energy 66 (2019) 104143, , https://doi.org/10.1016/j.nanoen.2019.104143.

[10] H. Liu, Q. Li, S. Zhang, R. Yin, X. Liu, Y. He, K. Dai, C. Shan, J. Guo, C. Liu, Electrically conductive polymer composites for smart flexible strain sensors: a critical review, J. Mater Chem. C 6 (2018) 12121–12141, https://doi.org/10.1039/C8TC04079F.

[11] R. Yin, S. Yang, Q. Li, S. Zhang, H. Liu, J. Han, C. Liu, C. Shen, Flexible conductive Ag nanowire/cellulose nanofibril hybrid nanopaper for strain and temperature sensing applications, Sci. Bull. (2020), https://doi.org/10.1016/j.scib.2020.02.020.

[12] S. Zhang, H. Liu, S. Yang, X. Shi, D. Zhang, C. Shan, L. Mi, C. Liu, C. Shen, Z. Guo, Ultrasensitive and highly compressible piezoresistive sensor based on polyurethane sponge coated with a cracked cellulose nanofibril/silver nanowire layer, ACS Appl. Mater. Interfaces 11 (2019) 10922–10932, https://doi.org/10.1021/acsami.9b00900.

[13] T. Kim, D. Kim, Y. Joo, J. Park, J. Yoon, Y. Hong, Crack propagation design in transparent polymeric conductive films via carbon nanotube fiber-reinforcement and its application for highly sensitive and mechanically durable strain sensors, Smart Mater. Struct. 28 (2018) 025008, , https://doi.org/10.1088/aaf0e9.

[14] T. Lee, Y.W. Choi, G. Lee, P.V. Pikhitsa, D. Kang, S.M. Kim, M. Choi, Transparent ITO mechanical crack-based pressure and strain sensor, J. Mater. Chem. C 4 (2016) 9947–9953, https://doi.org/10.1039/c6tc03329f.

[15] C. Luo, J. Jia, Y. Gong, Z. Wang, Q. Fu, C. Pan, Highly Sensitive, Durable, and multifunctional sensor inspired by a spider, ACS Appl. Mater. Interfaces 9 (2017) 19955–19962, https://doi.org/10.1021/acsami.7b02988.

[16] E. Oh, T. Kim, J. Yoon, S. Lee, D. Kim, B. Lee, J. Byun, H. Cho, J. Ha, Y. Hong, Highly reliable liquid metal-solid metal contacts with a corrugated single-walled carbon nanotube diffusion barrier for stretchable electronics, Adv. Funct. Mater. 28 (2018) 1806014, , https://doi.org/10.1002/adfm.201806014.

[17] S. Kim, J. Byun, S. Choi, D. Kim, T. Kim, S. Chung, Y. Hong, Negatively strain-dependent electrical resistance of magnetically arranged nickel composites: application to highly stretchable electrodes and stretchable lighting devices, Adv. Mater. 26 (2014) 3094–3099, https://doi.org/10.1002/adma.201304686.

[18] J. Lee, S. Chung, H. Song, S. Kim, Y. Hong, Lateral-crack-free, buckled, inkjet-printed silver electrodes on highly pre-stretched elastomeric substrates, J. Phys. D Appl. Phys. 46 (2013) 105305, , https://doi.org/10.1088/0022-3727/46/10/105305.

[19] Y. Kim, X. Ren, J.W. Kim, H. Noh, Direct inkjet printing of micro-scale silver electrodes on polydimethylsiloxane (PDMS) microchip, J. Micromech. Microeng. 24 (2014) 115010, , https://doi.org/10.1088/0960-1317/24/11/115010.

[20] J. Byun, E. Oh, B. Lee, S. Kim, S. Lee, Y. Hong, A Single Droplet-Printed Double-Side Universal Soft Electronic Platform for Highly Integrated Stretchable Hybrid Electronics, Adv. Funct. Mater. 27 (2017) 1701912, , https://doi.org/10.1002/adfm.201701912.

[21] J. Byun, B. Lee, E. Oh, H. Kim, S. Kim, S. Lee, Y. Hong, Fully printable, strain-engineered electronic wrap for customizable soft electronics, Sci. Rep. 7 (2017) 45328, https://doi.org/10.1038/srep45328.

[22] S. Chung, J. Lee, H. Song, S. Kim, J. Jeong, Y. Hong, Inkjet-printed stretchable silver electrode on wave structured elastomeric substrate, Appl. Phys. Lett. 98 (2011) 153110, , https://doi.org/10.1063/1.3578398.

[23] A. Kim, J. Ahn, H. Hwang, E. Lee, J. Moon, A pre-strain strategy for developing a highly stretchable and foldable one-dimensional conductive cord based on a Ag nanowire network, Nanoscale 9 (2017) 5773–5778, https://doi.org/10.1039/c7nr02116j.

[24] K.K. Kim, S. Hong, H.M. Cho, J. Lee, Y.D. Suh, J. Ham, S.H. Ko, Highly Sensitive and Stretchable Multidimensional Strain Sensor with Prestrained Anisotropic Metal Nanowire Percolation Networks, Nano Lett. 15 (2015) 5240–5247, https://doi.org/10.1021/acs.nanolett.5b01505.

[25] T.T. Yang, X.M. Li, X. Jiang, S.Y. Lin, J.C. Lao, J.D. Shi, Z. Zhen, Z.H. Li, H.W. Zhu, Structural engineering of gold thin films with channel cracks for ultrasensitive strain sensing, Mater Horiz. 3 (2016) 248–255, https://doi.org/10.1039/c6mh00027d.

[26] M. Amjadi, M. Turan, C.P. Clementson, M. Sitti, Parallel microcracks-based ultrasensitive and highly stretchable strain sensors, ACS Appl. Mater. Interfaces 8 (2016) 5618–5626, https://doi.org/10.1021/acsami.5b12588.

[27] S.M. Zhang, L. Cai, W. Li, J.H. Miao, T.Y. Wang, J. Yeom, N. Sepulveda, C.A. Wang, Fully printed silver-nanoparticle-based strain gauges with record high sensitivity, Adv. Electron. Mater. 3 (2017) 1700067, , https://doi.org/10.1002/aelm.201700067.

[28] C.J. Lee, K.H. Park, C.J. Han, M.S. Oh, B. You, Y.S. Kim, J.W. Kim, Crack-induced Ag nanowire networks for transparent, stretchable, and highly sensitive strain sensors, Sci. Rep. 7 (2017) 7959, https://doi.org/10.1038/s41598-017-08484-y.

[29] H.N. Kim, S.H. Lee, K.Y. Suh, Controlled mechanical fracture for fabricating microchannels with various size gradients, Lab Chip 11 (2011) 717–722, https://doi.org/10.1039/c0lc00277a.

[30] Y.H. Wu, H.Z. Liu, S. Chen, X.C. Dong, P.P. Wang, S.Q. Liu, Y. Lin, Y. Wei, L. Liu, Channel Crack-Designed Gold@PU sponge for highly elastic piezoresistive sensor with excellent detectability, Acs Appl. Mater. Inter. 9 (2017) 20098–20105, https://doi.org/10.1021/acsami.7b04605.

[31] Z. Liu, D. Qi, P. Guo, Y. Liu, B. Zhu, H. Yang, Y. Liu, B. Li, C. Zhang, J. Yu, B. Liedberg, X. Chen, Thickness-gradient films for high gauge factor stretchable strain sensors, Adv. Mater. 27 (2015) 6230–6237, https://doi.org/10.1002/adma.201503288.

[32] J. Park, I. You, S. Shin, U. Jeong, Material approaches to stretchable strain sensors, ChemPhysChem 16 (2015) 1155–1163, https://doi.org/10.1002/cphc.201402810.

[33] T. Yamada, Y. Hayamizu, Y. Yamamoto, Y. Yomogida, A. Izadi-Najafabadi, D.N. Futaba, K. Hata, A stretchable carbon nanotube strain sensor for human-motion detection, Nat. Nanotechnol. 6 (2011) 296–301, https://doi.org/10.1038/nnano.2011.36.

[34] D.J. Lipomi, M. Vosgueritchian, B.C. Tee, S.L. Hellstrom, J.A. Lee, C.H. Fox, Z. Bao, Skin-like pressure and strain sensors based on transparent elastic films of carbon nanotubes, Nat. Nanotechnol. 6 (2011) 788, https://doi.org/10.1038/nnano.2011.184.

[35] Y.-Q. Li, P. Huang, W.-B. Zhu, S.-Y. Fu, N. Hu, K. Liao, Flexible wire-shaped strain sensor from cotton thread for human health and motion detection, Sci. Rep. 7 (2017) 1–7, https://doi.org/10.1038/srep45013.